

## TWO-PHASE FRICTIONAL PRESSURE DROP OF R245fa IN A 1.1 MM TUBE

Jaqueline Diniz da Silva, [jaqueline@sc.usp.br](mailto:jaqueline@sc.usp.br)  
Cristiano Bigonha Tibiriçá, [bigonha@sc.usp.br](mailto:bigonha@sc.usp.br)  
Gherhardt Ribatski, [ribatski@sc.usp.br](mailto:ribatski@sc.usp.br)

Escola de Engenharia de São Carlos, University of São Paulo, Av. Trabalhador São Carlense, 400, São Carlos, SP, Brazil

**Abstract.** This work presents new experimental flow boiling pressure drop results for a horizontal smooth tube of 1.1 mm ID using R245fa as working fluid. The experimental data were performed under adiabatic conditions, mass velocities from 100 to 700 kg/m<sup>2</sup>s, heat flux in the range from 10 to 100kW/m<sup>2</sup>, saturation temperatures of 22 and 31°C and exit vapor qualities up to 0.99. The study analyzed the heat transfer and pressure drop based on previous data and literature. Five frictional pressure drop predictive methods were compared against the experimental database. The method by Cioncolini et al. (2009) provided quite accurate predictions of the present database.

**Keywords:** Pressure drop, Microchannel, Two-Phase Flow

### INTRODUCTION

In recent years, emphasis has been put on the characteristics of microscale two-phase flow systems which have interest by the industrial demand for compact devices capable of dissipating extremely high heat fluxes such as microelectronic cooling system and solar power ‘concentrators’. Despite the enormous benefits that can be achieved by using precise designing methods, they are still not available and flow boiling based heat spreaders have been developed based on prototype machining and testing.

To evaluate the ability of available methods to predict two-phase flow pressure drop in microscale channels, Felcar and Ribatski (2008) compared 17 pressure drop macro- and microscale predictive methods against a database comprising experimental data from 15 independent laboratories. They found that the homogeneous model with the dynamic viscosity according to Cicchitti et al. (1960) provides the best predictions of the overall database. According to Felcar and Ribatski (2008), despite of being the best, Cicchitti et al. (1960) method failed to predict most of the databases. In their study, Felcar and Ribatski (2008) have also performed comparisons of the predictive methods and the experimental results segregated according to flow patterns by using the micro-scale flow pattern predictive method previously proposed by Felcar et al. (2007). From this analysis, they pointed out conclusions similar to those obtained for the overall database. Ribatski et al. (2006) have also performed comparisons of the predictive methods and experimental results from literature for the overall database and for the data segregated according to flow patterns. They presented conclusions similar to those indicated by Felcar and Ribatski (2008).

According to Tibiriçá and Ribatski (2010), for R245fa and Tibiriçá et al. (2011) for R134a, both studies in a 2.3 mm ID tube, the frictional pressure drop increases with increasing mass velocity and vapor quality and decreasing saturation temperature. Heat flux has a negligible effect on the two-phase frictional pressure drop.

In order to evaluate the accuracy of the pressure drop predictive methods, in this paper new frictional pressure drop data in a 1.1 mm ID horizontal stainless steel tube 160 mm long are compared against the leading predictive methods. Moreover, this data are carefully analyzed and compared against previous results obtained by our group.

### EXPERIMENTS

#### 2.1. Test apparatus and experimental procedure

The experimental setup is comprised of refrigerant and ethylene-glycol circuits. In the refrigerant circuit (see Fig. 1), starting from the sub cooler 1, the test fluid flows through the filter to the micropump. Downstream the micropump, a bypass piping line containing a needle-valve is installed so that together with a frequency controller on the micropump the desired liquid flow rate can be set. There is then a Coriolis mass flow meter and the sub cooler 2 to assure that the fluid entering the pre-heater is sub cooled. Just upstream the pre-heater inlet, the liquid enthalpy is estimated from its temperature T1 by a 0.125mm thermocouple within the pipe connection and its pressure p1 by an absolute pressure transducer.

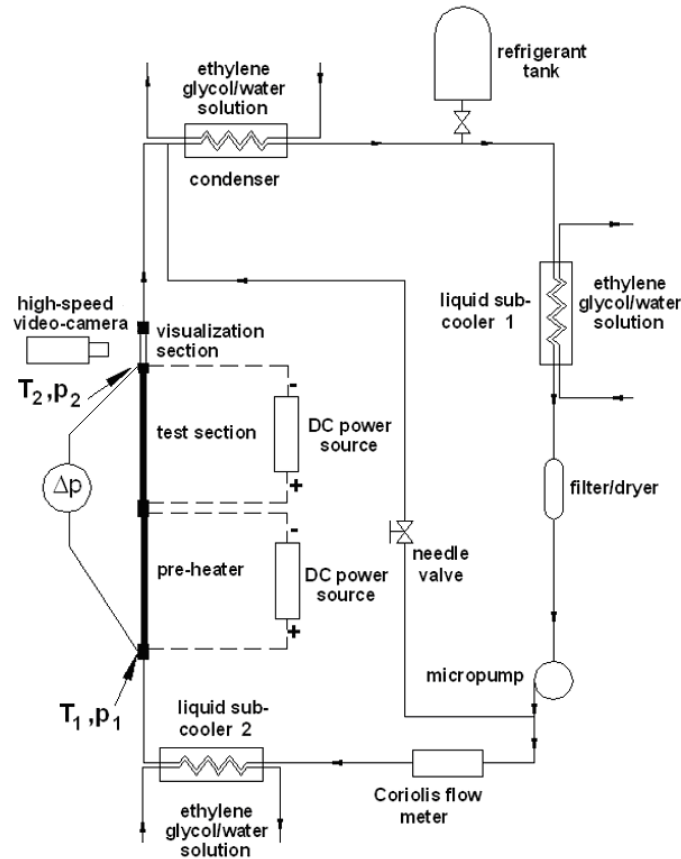


Figure 1. Schematic diagram of the refrigerant circuit.

At the pre-heater, the fluid is heated up to the desired condition at the test section inlet. The pre-heater and the test section are horizontal stainless steel tubes with an internal diameter of 1.1 mm and 160 mm long. The pre-heater and the test section are thermally insulated. Their internal surface roughness was measured by a surface profiler using an open tube and a value of  $0.67 \mu\text{m}$  was found for the mean absolute roughness,  $R_a$ . The pre-heater is heated by applying direct current (DC) to its surface. The power is supplied to the pre-heater by a DC power source. The visualization section is a horizontal fused silica tube with an inner diameter of 1.1 mm, a length of 100 mm, and is located just downstream to the test section. The pre-heater, the test section and the flow visualization section are connected through junctions made of electrical insulation material. Once the liquid leaves the test section its temperature  $T_2$  is determined from a 0.125 mm thermocouple within the pipe. The corresponding absolute pressure is estimated from a differential pressure transducer that gives the total pressure drop between the pre-heater inlet and the test section outlet,  $\Delta p$ . Then, the working fluid is directed to the tube-in-tube type heat exchanger where it is condensed and subcooled. The refrigerant tank containing a serpentine coil operates as a reservoir of the working fluid and is used to control the saturation pressure in the refrigerant circuit. The saturation pressure is set by adjusting the temperature of the anti-freezing ethylene glycol aqueous solution that flows through the serpentine coil within the tank.

Wall temperatures are measured through 0.125 mm type K thermocouples fixed along the test section. The thermocouples were placed on the surface by firmly pressuring them against the tube wall using a special apparatus developed by the group resulting in a smaller thermal contact resistance between the thermocouples and the tube wall. At each measuring cross-section, the surface temperature is read at four locations (on right and left sides, bottom and top) as indicated in Fig. 2.

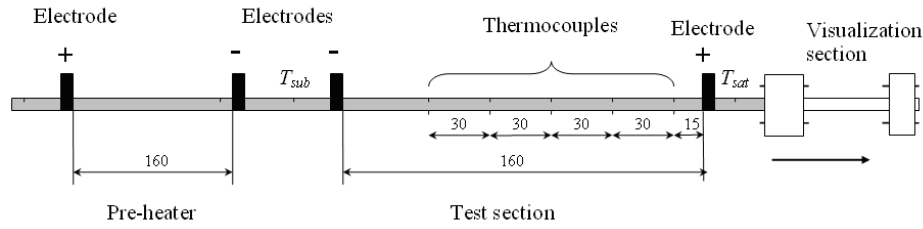


Figure 2. Details of the test section and thermocouples positioning along its surface.

The experiments were conducted first by setting the temperature in the refrigerant tank. Once established the saturation pressure in the refrigerant circuit by controlling the temperature in the refrigerant tank, the mass velocity was set through a frequency controller acting on the micropump. Then, the desired vapor quality at the test section inlet is imposed by varying the power supplied to the pre-heater. Experimental results are obtained for distinct vapor qualities, keeping the remaining parameters fixed. The datum points were logged only under steady-state conditions characterized by temperature, pressure and mass flow measurement variations within the error range of the instrument.

## 2.2. Data reduction procedure

Firstly, the subcooled region length, the single-phase pressure drop over its length, and the saturation temperature at the beginning of the saturated region were calculated. They were estimated based on the heat flux and the measured temperature and pressure at the pre-heater inlet by solving simultaneously an equation of state from EES, Equation Engineering Solver, (Klein, 2007) relating  $P_{sat}$  and  $T_{sat}$  plus energy balance and single-phase pressure drop equations. The overall pressure drop over the saturated region was then determined by subtracting the single-phase pressure drop from the measured total pressure drop,  $\Delta p$ .

The heat flux,  $q$ , was calculated as the ratio between the electrical power supplied to the test section and its internal area based on the heated length, where the electrical power was given by the product between the electrical current and voltage supplied by the DC power source.

The inlet vapour quality was determined by an energy balance over the pre-heater according to the following equation:

$$x_{out} = \frac{1}{i_{lv,out}} \left[ \frac{4(P_1)}{G \pi D^2} + (i_{l,in} - i_{l,out}) \right] \quad (1)$$

The enthalpy of the liquid at the inlet of the pre-heater,  $i_{l,in}$ , was estimated based on the measured temperature  $T_1$  and pressure  $p_1$ . The liquid enthalpy and the latent heat of vaporization at the visualization section ( $i_{l,out}$  and  $i_{lv,out}$ , respectively) were estimated based on the fluid temperature measured just downstream of the test section,  $T_2$ , and saturated state was assumed. In Eq. (1),  $P_1$  is the electrical power supplied by the DC power source to the pre-heater.

Adiabatic horizontal pressure drop gradients were estimated from the temperature readings of the thermocouples attached to the test section outer surface as showed in Fig. 3. Pressure drop measurements using a similar procedure were already successfully performed by Revellin and Thome (2007). In order to apply such a procedure, thermodynamic equilibrium between the phases was assumed. It was also adopted that the fluid saturation temperature in a specific axial position along the test section length is the same as the local perimeter-averaged wall temperature. So, the local saturation pressure can be estimated from the wall temperature measurements. The adiabatic pressure drop gradients were estimated over a tube length of 160 mm.

## 2.3. Experimental validation

Single-phase flow experiments were performed in order to assure the accuracy of the estimated vapour quality and evaluate the effective rate of heat losses during single-phase experiments,  $(\Delta E/E)$ , defined as follows:

$$\left(\frac{\Delta E}{E}\right) = \frac{\left[\left(\frac{\pi D^2}{4}\right) G(i_{out} - i_{in})\right] - (P_1 + P_2)}{P_1 + P_2} \quad (4)$$

where  $i_{in}$  and  $i_{out}$  are the refrigerant enthalpies estimated at the pre-heater inlet and just downstream the test section, respectively.  $P_2$  is the electrical power supplied by the DC power source to the test section. The single phase heat losses were always less than 10% with an average of 6%.

Temperature measurements were calibrated and the temperature uncertainty evaluated according to the procedure suggested by Abernethy and Thompson (1973). Uncertainties for the calculated parameter were estimated using the method of sequential perturbation according to Moffat (1988). The experimental uncertainties are listed in Table 1. Table 1 presents the uncertainties of the measured and calculated parameters, including the maximum uncertainties of the heat transfer coefficient and vapor quality. To calculate the uncertainties of the estimated vapor qualities, heat losses of 5% were assumed. Such a procedure was adopted since for  $T_{exit}=31$  °C and high mass velocities, single phase heat losses were about 5%. It should be mentioned that during two-phase flow, heat losses are much smaller than during single-phase flow due to a much higher internal heat transfer coefficient. In order to calculate the heat transfer coefficient uncertainties, heat losses to the environment were neglected due to the same abovementioned reason. Effects of axial heat conduction along the tube length, at the cross sections where wall temperatures were measured, were found negligible.

Table 1. Uncertainty of measured and calculated parameters

Parameter	Uncertainty	Parameter	Uncertainty
$D$	20 $\mu\text{m}$	$p$	2 kPa
$L$	1 mm	$\Delta p$	150 Pa
$G$	1.7%	$P_1, P_2$	0.88%
$x$	<5%	$T$	0.15 °C

### 3. EXPERIMENTAL RESULTS

A parametric investigation of the effect of the experimental variables on the two-phase frictional pressure drop is presented. Experiment conditions and fluid properties are displayed in Table 2.

Table 2. Experiment conditions, and fluid properties.

$G$	$x$	$q$	$T$	$\Delta p$	$T$	$D$	Tube	Ra	Fluid
$\text{kg/m}^2\text{s}$	(%)	$\text{kW/m}^2$	°C	$\text{kPa/m}$	°C	(mm)	$\mu\text{m}$		
100-700	20-99	10-100	31	1-48	31	1.1	.037		R245fa

R245fa properties	$T$	$P$	$\rho_l$	$\rho_v$	$h_v$	$\mu_l$	$k_l$	$\sigma$
	(°C)	(MPa)	( $\text{kg/m}^3$ )	( $\text{kg/m}^3$ )	( $\text{kJ/kg}$ )	( $\mu\text{Pa}\cdot\text{s}$ )	( $\text{mW/m}\cdot\text{K}$ )	( $\text{mN/m}$ )
	31	0.8	1320	8.7	240.6	373.9	79.4	7.3

where  $G$  is mass velocity ( $\text{kg m}^{-2}\text{s}^{-1}$ ),  $\rho_l$  is density of liquid phase ( $\text{kg m}^{-3}$ ),  $\rho_g$  is density of vapour phase ( $\text{kg m}^{-3}$ ),  $\sigma$  is surface tension ( $\text{N m}^{-1}$ ),  $\mu_l$  is viscosity of liquid phase,  $k_l$  is conductivity of liquid phase.

Figure 3 shows the effect of mass velocity and vapour quality on the frictional pressure drop during adiabatic flows. As already expected, the frictional pressure drop increases with increasing mass velocity. In this figure, a pressure drop peak at higher vapour qualities is not displayed probably due to the fact that the experiments were performed for lower vapour qualities. The displayed behaviours are not new and are similar to those observed in macro-scale channels (see Moreno-Quibén *et al.* (2007)) and in most of the studies concerning micro-scale channels as the results displayed in Fig. 4 by Tibiriçá and Ribatski (2010) for R245fa in a 2.3 mm tube. By comparing Figs. 3 and 4, it can be noticed as expected that the pressure drop increases drastically with decreasing the tube diameter from 2.3mm to 1.1mm.

The adiabatic two-phase experimental pressure drop data points were compared against four frictional pressure drop prediction methods. The new prediction methods of Cioncolini *et al.* (2009) and Sun and Mishima (2009) were evaluated in addition to the homogeneous model, using Cicchitti *et al.* (1960) two-phase viscosity, Müller-Steinhagen

and Heck (1986) correlation and Lockhart and Martinelli (1949) model with the Chisholm (1973) constant. Mean absolute error,  $\varepsilon$ , was used as the criterion to evaluate the correlations.

Figures 5 to 9 display comparisons of the experimental data and the predictive methods. As general, Cioncolini *et al.* (2009) was classified as the best method with  $\varepsilon = 11.1\%$ . Müller-Steinhagen and Heck (1986) was ranked as the second best, followed by Homogeneous model and Lockhart and Martinelli (1949). Curiously, the method by Lockhart and Martinelli (1949) developed for large diameter tubes gives also reasonable predictions. As abovementioned, it is expected that tube diameters between 1 and 4 mm are within a range where transitional flow pattern, pressure drop and heat transfer behaviors seem to occur. This can result that both macro- and micro-scale methods works relatively well within this range of diameters depending on the fluid. Figure 9 also shows the evolution of the frictional pressure drop data with vapor quality according to the experimental results and predictive methods. According to this figure, Cioncolini *et al.* (2009) method is not only statistically accurate but that it also properly captures the trends in the frictional pressure drop data.

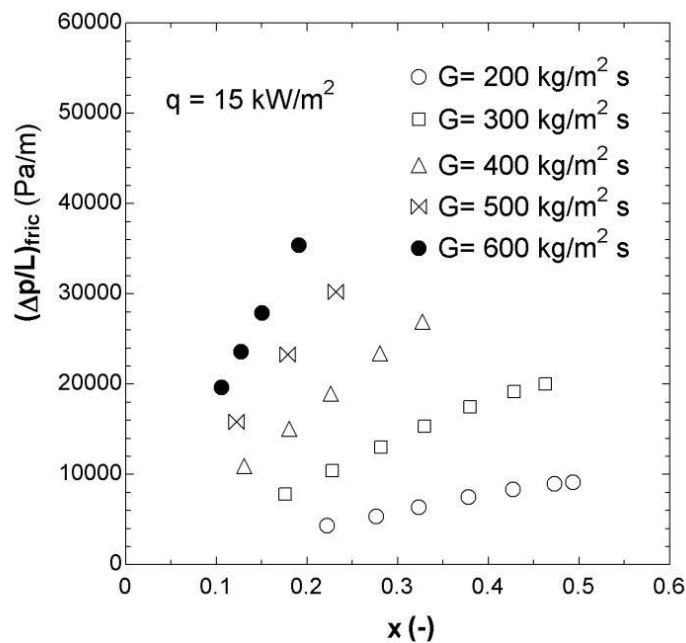


Figure 3. Mass velocity and vapor quality effects on the frictional pressure drop for  $T_{sat} = 31\text{ }^{\circ}\text{C}$ .

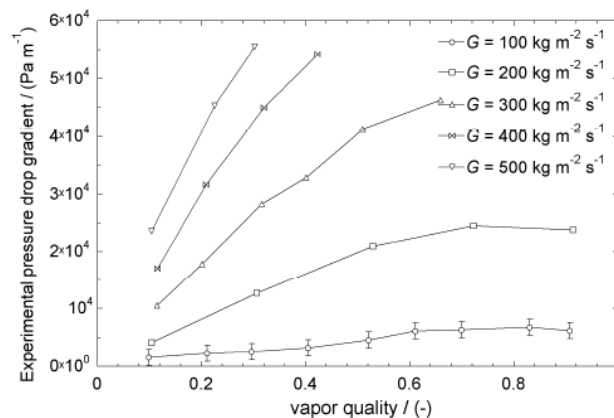


Figure 4- mass velocity effect on the frictional pressure drop for two-phase flow of R245fa in a 2.3 mm ID tube. Tibiriçá and Ribatski (2010)

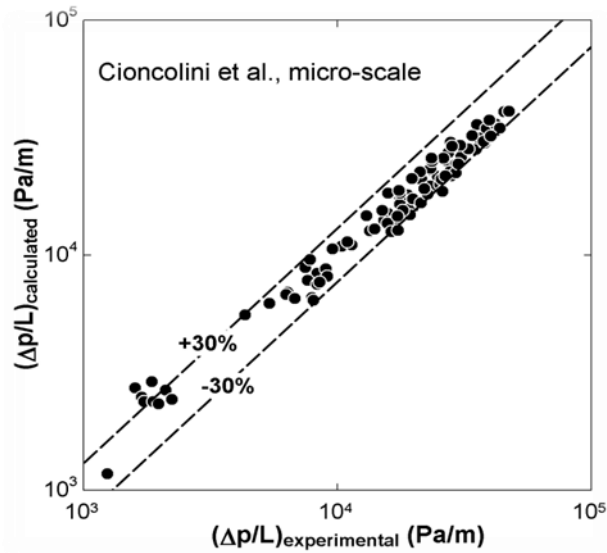


Figure 5. Comparison of the experimental data and the Cioncolini *et al.* (2009) predictive method for micro-scale channels.

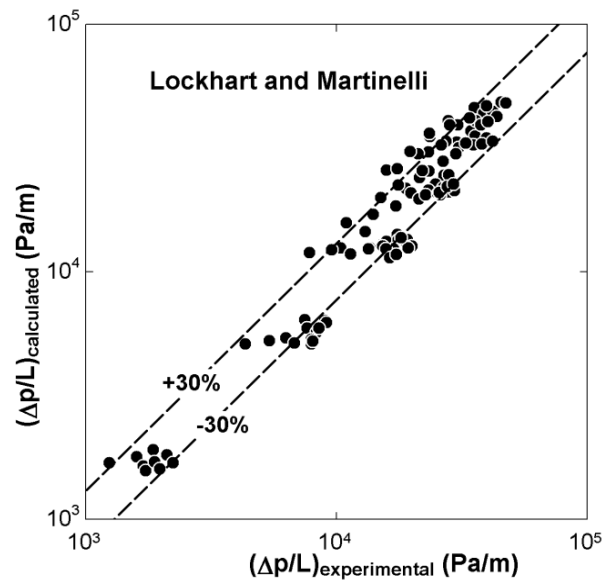


Figure 6. Comparison of the experimental data and the Lockhart and Martinelli (1949) predictive method.

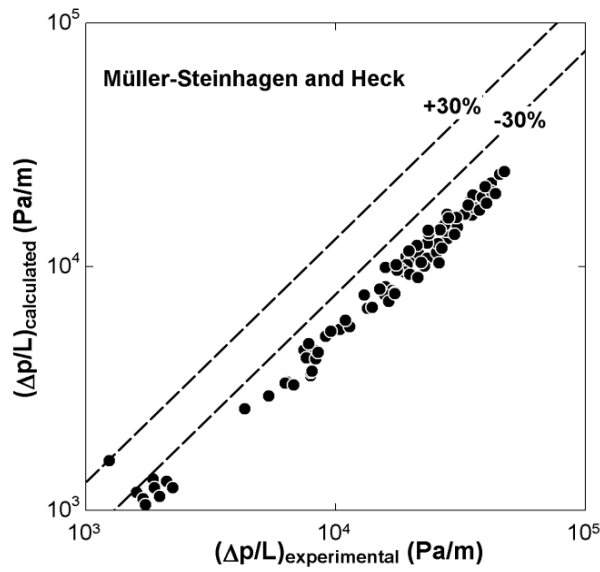


Figure 7. Comparison of the experimental data and the Müller-Steinhagen and Heck (1986) predictive method.

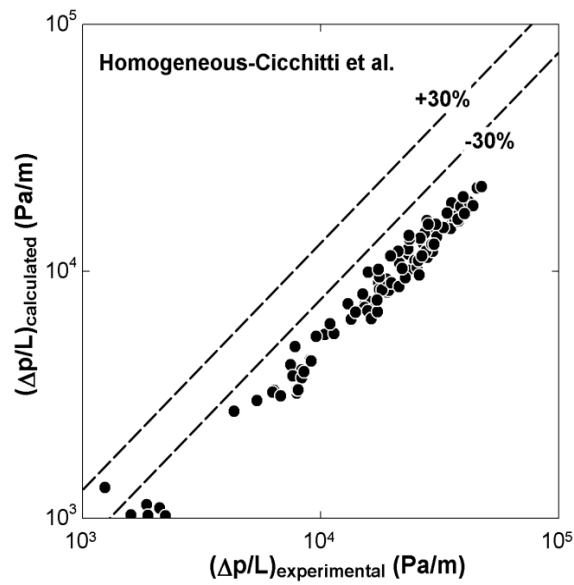


Figure 8. Comparison of the experimental data and the homogeneous model with the two-phase viscosity proposed by Cicchitti et al. (1960).

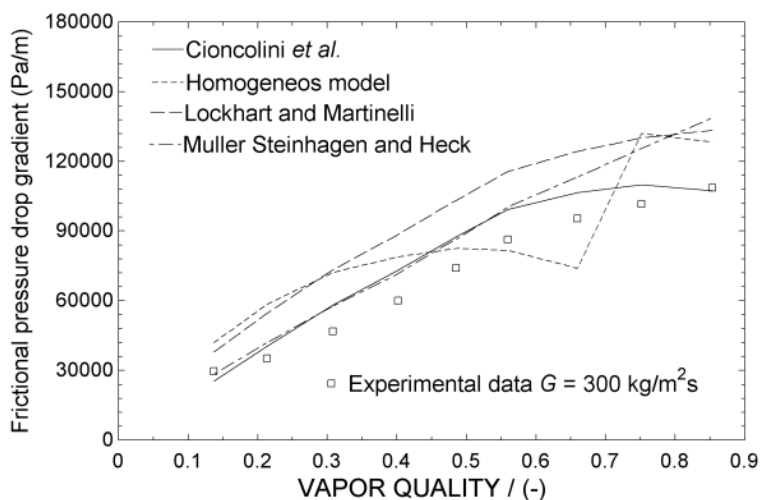


Figure 9. Comparison of adiabatic pressure drop data and prediction methods.

#### 4. CONCLUSIONS

New accurate micro-scale frictional pressure drop data for R245fa in a 1.1mm circular channel were obtained. The experimental data were analyzed and compared against predictive methods. The frictional pressure drop increases with increasing mass velocity and vapor quality. The predictive methods of Cioncolini *et al.* (2009) worked the best for adiabatic data with a mean average error 11.1%.

#### 5. ACKNOWLEDGMENT

The authors gratefully acknowledge the financial support under contract numbers 05/60031-0, 06/52089-1 and 07/53950-5 given by FAPESP (The State of São Paulo Research Foundation, Brazil), Contract No. DS 00011/07-0 by CAPES Brazilian Federal Agency for Support and Evaluation of Graduate Education and NANOBIOTEC given by CAPES. The technical support given to this investigation by Mr. José Roberto Bogni is appreciated and recognized.

#### 7. REFERENCES

- Cioncolini, A., Thome, J. R., Lombardi, C. 2009, Unified macro-to-microscale method to predict two-phase frictional pressure drops of annular flows, *Int. J. Multiphase Flow* 35: 1138-1148.
- Felcar, H. O., and Ribatski, G., 2008, "Avaliação de métodos preditivos para perda de carga durante o escoamento bifásico e a ebulição convectiva em micro-canais," Proceedings of the First Brazilian Meeting on Boiling, Condensation and Multiphase Flow, Florianópolis, Brazil, Paper No. MF-104.
- Felcar, H.O.M., Ribatski, G., Saiz-Jabardo, J.M., 2007, "A Gas-Liquid Flow Pattern Predictive Method for Macroand Mini-Scale Round Channels", Proc. 10th UK Heat Transfer Conference, Edinburgh, Scotland.
- Cicchitti, A., Lombardi, C., Silvestri, M., Soldaini, G., and Zavattarelli, R., 1960, "Two-Phase Cooling Experiments Pressure Drop, Heat Transfer and Burnout Experiments," *Energia Nucleare*, 7, pp. 407-425.
- Ribatski, G., Wojtan, L., Thome, J. R. 2006, An analysis of experimental data and prediction methods for two-phase frictional pressure drop and flow boiling heat transfer in micro-scale channels, *Exp. Thermal Fluid Science* 31: 1-19.
- Tibiriçá, C. B., and Ribatski, G., "Two-Phase Frictional Pressure Drop and Flow Boiling Heat Transfer for R245fa in a 2.3 mm Tube," *Heat Transfer Eng.*, in press.
- Klein, S.A. 2007, Engineering Equation Solver (EES), Academic Professional Version.
- Revellin, R., Thome, J. R. 2007, Adiabatic two-phase frictional pressure drops in micro-channels, *Exp. Thermal Fluid Science* 31: 673-685.
- Abernethy, R.B., and Thompson, J.W., 1973. Handbook uncertainty in gas turbine measurements, Arnold Engineering Development Center, Arnold Air Force Station, Tennessee.
- Moffat, R.J., 1988. Describing the uncertainties in experimental results, *Exp. Thermal Fluid Science*, vol. 1, pp. 3-17.
- Moreno-Quibén, J. M., Lima, R. J. S., Thome, J. R. 2007, Flow pattern based two-phase frictional pressure drop model for horizontal tubes. Part I: Diabatic and adiabatic experimental study, *Int. J. Heat and Fluid Flow* 28(5): 1049-1059.

- Müller-Steinhagen, H., Heck, K. 1986, A simple friction pressure drop correlation for two-phase flow in pipes, Chem. Eng. Process 20: 297-308.
- Lockhart, R. W., Martinelli, R. C., 1949, "Proposed correlation of data for isothermal two-phase, two-component flow in pipes", Chem. Eng. Progr, 45, pp. 39 - 48.

## **8. RESPONSIBILITY NOTICE**

The authors are the only responsible for the printed material included in this paper.